Eur. Phys. J. A **20**, 157–162 (2004)
DOI 10.1140/epja/i2002-10343-x

THE EUROPEAN PHYSICAL JOURNAL A

Study of thermally excited nuclei through E1 and E2 decay from collective modes

B. Million[1,a], A. Bracco[1], G. Benzoni[1], S. Leoni[1], F. Camera[1], O. Wieland[1], A. Maj[2], M. Kmiecik[2], A. Gadea[3], and B. Herskind[4]

[1] Dipartimento di Fisica, Università di Milano and INFN, via Celoria 16, 20133 Milano, Italy
[2] Niewodniczanski Institute of Nuclear Physics, 31-342 Krakow, Poland
[3] Laboratori Nazionali di Legnaro, via Romea, Legnaro (PD), Italy
[4] The Niels Bohr Institute, Blegdamsvej, 15-17, 2100 Copenhagen, Denmark

Received: 2 December 2002 /
Published online: 2 March 2004 –

Abstract. The nuclear system at the limit of excitation energy and angular momentum is here studied in the case of the superdeformed nucleus ^{143}Eu using γ-spectroscopy techniques. The data are based on a EUROBALL experiment using the reaction $^{37}\mathrm{Cl} + {}^{110}\mathrm{Pd} \rightarrow {}^{143}\mathrm{Eu} + 4\mathrm{n}$. The influence of thermal energy on superdeformed configurations is investigated through the analysis of the quasi-continuum spectra formed by $E2$ transitions among states of excited rotational bands with energy extending up to 4-5 MeV above the yrast line. In particular, the effective lifetimes of the discrete rotational bands forming ridge structures in γ-γ coincidence matrices is measured by a Doppler Shift Attenuation Method. The deduced quadrupole deformation of $Q_t \approx 10$ eb indicates that the nucleus maintains its collectivity with increasing excitation energy, supporting the superdeformed character of the excited nuclear rotation. The obtained number of superdeformed discrete bands forming the ridge structures is found in good agreement with microscopic cranked shell model calculations including the decay-out process into the lower deformation minimum. In addition, the nuclear properties at higher excitation energies are investigated through the $E1$ γ-decay of the giant dipole resonance (GDR). It is found that the intensity of the superdeformed yrast and excited bands increases by a factor of approximately 1.6 when a coincidence with a high-energy γ-ray is required, showing the importance of the $E1$ cooling in the feeding mechanism of the superdeformed states.

PACS. 21.10.Tg Lifetimes – 21.10.Re Collective levels – 23.20.Lv γ transitions and level energies – 27.60.+j $90 \leq A \leq 149$

1 Introduction

In the last years, the focus of many experiments with large γ-detector arrays has been the study of exotic nuclear shapes, particularly of superdeformed (SD) type and of the mechanism leading to their population and decay-out. We now know that the very existence of such weakly populated structures is made possible by the presence of different nuclear shapes, which can coexist over a wide spin range, being well separated by a potential energy barrier in the deformation space [1]. This also explains the sudden decay-out of the SD rotational bands as a tunnelling process through the barrier which separates the superdeformed (SD) and the normal deformed (ND) minima. Such scenario can now be studied not only in the case of the SD yrast, but also in connection with SD excited rotational states, forming quasi-continuous ridge-valley structures in γ-γ coincidence spectra. This is due to both the higher sensitivity of the latest generation multi detector Ge-arrays and to recently developed theoretical calculations which are able to describe the thermally excited rotational motion and the barrier penetration effect.

In the present paper we focus on the experimental study of the properties of the thermally excited rotational bands in the superdeformed nucleus ^{143}Eu, up to the region of rotational damping. In particular, making use of the EUROBALL array, we measure for the first time the effective lifetime of the excited rotational bands forming the ridge structure in γ-γ coincidence matrices. The obtained results, consistent with the quadrupole deformation $Q_t \approx 10$ eb, support the strong collective character of the excited discrete rotational states [2]. The number of excited rotational bands populating the ridges is also measured by a statistical analysis of the fluctuations in the number of counts of γ-γ coincidence spectra. This number

[a] e-mail: million@mi.infn.it

will be compared with microscopic cranked shell model calculations [3,4] including the decay-out mechanism into the ND well, in a similar way as it was modelled for the SD yrast [5,6]. This allows to probe the quantum tunnelling of the thermally excited SD rotational states, and also supports the band mixing model, and also to test in detail the band mixing model.

The problem of the population of the superdeformed configurations is also studied by investigating the cooling of the residual nucleus by statistical $E1$. In fact, it has been predicted that one of the components of the giant dipole resonance built on very elongated shapes will be shifted to low energy, therefore strongly affecting the $E1$ transition probability and consequently the population of the SD states [7]. With the present data the intensity of the superdeformed yrast and excited bands is investigated when measured in coincidence with a high-energy γ-ray, to determine the importance of the $E1$ cooling in the feeding mechanism of the superdeformed states [8].

2 Experimental information

The experiment was performed at the Tandem Accelerator Laboratory of Legnaro (Padova, Italy). The nucleus ^{143}Eu was populated by the fusion reaction ^{37}Cl + ^{110}Pd $\rightarrow$^{143}Eu + 4n, at a beam energy of 165 MeV. This bombarding energy is 5 MeV larger than the one giving the maximum population of the SD yrast band and it was chosen to allow for a large enough available phase space for $E1$ emission from the final residual nucleus. The maximum angular momentum is predicted to be 68 $\hbar$ by the heavy-ion grazing model [9]. The target of ^{110}Pd (97.3% pure and 950 μg/cm^2 thick) was evaporated on a Au backing of 15 mg/cm^2. Low-energy γ-rays were detected in the EUROBALL array [10], where the thirty tapered Ge detectors in the forward hemisphere were replaced by the eight large-volume BaF_2 scintillators of the HECTOR detector for high-energy detection [11]. They were placed at 30 cm from the target to allow for a good neutron rejection by time-of-flight measurement relative to four additional small BaF_2 detectors, used as a time reference. The gain of each of the large-volume BaF_2 has been monitored continuously during the measurement with a LED source and small shifts were corrected during the off-line analysis. The EUROBALL germanium detectors were calibrated with standard radioactive sources, while the large volume scintillators were calibrated with the reaction $^{11}\mathrm{B} + \mathrm{D} \rightarrow {}^{12}\mathrm{C}^* + \mathrm{n}$ which emits a 15.1 MeV γ-ray. Events with coincidences among at least 3 Ge detectors (without Compton suppression) and an additional coincidence with a high-energy γ-ray (larger than 3 MeV) measured in the BaF_2 detectors were registered. A total of 1.4×10^9 Ge events with average fold 3 was collected after the Compton suppression and the application of an energy-dependent time gate to reject neutron-induced peaks. It is found that more than 60% of the total statistics of the experiment leads to the final residue ^{143}Eu.

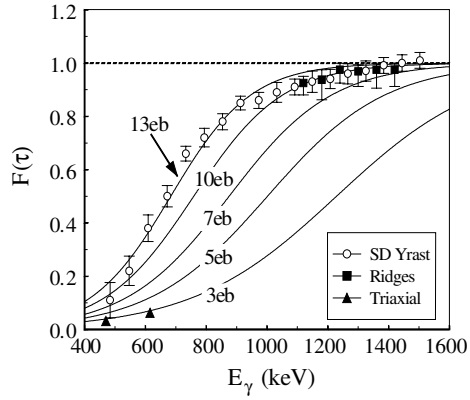

Fig. 1. The measured fractional Doppler shift for the superdeformed yrast (circles) [12], the triaxial transitions (triangles) [13] and the superdformed ridges (squares) [2] of ^{143}Eu. The lines represent the expected theoretical values for Q_t = 3, 5, 7, 10 and 13 eb (from ref. [2]).

3 Lifetime measurements of the unresolved discrete structures

In order to measure the quadrupole moment associated to the unresolved excited rotational bands forming the $E2$ quasi-continuum, a lifetime measurement employing the DSAM technique has been made. In particular, we have focused on the ridge structure which is in this nucleus characterized by a moment of inertia very similar to that of the SD yrast line. To take advantage of the entire statistics of the experiment, an energy-dependent Doppler correction, corresponding to a given quadrupole deformation Q_t, has been applied to the backed target data on an event-by-event basis. In this way, a number of matrices have been created, each for a different Q_t varying from 3 eb to 13 eb, and analyzed [2]. The best Q_t value deduced from the analysis is comprised between 10 and 13 eb, as illustrated in fig. 1. In the figure, previous measurements of the fractional Doppler shift for the SD yrast transitions (circles) [12] are also shown, together with values for two transitions of the co-existing triaxial configuration (triangles) [13], and with the calculations from ref. [12]. One should note that in the triaxial case, which is the second largest deformed shape of ^{143}Eu after the SD one, the fractional Doppler shift is very different and corresponds to a quadrupole moment Q_t of about 3 eb. It is found that the experimental results for both SD yrast and ridge structures are in agreement with a quadrupole moment of the order of $\approx$ 10 eb for $E_\gamma > 1000$ keV, indicating that the nucleus ^{143}Eu maintains its collectivity and deformation with increasing excitation energy, as also observed in normally deformed nuclei [14,15].

4 Quantum tunnelling of excited superdeformed bands

An interesting information than can be deduced from the analysis of the ridge structure using the fluctuation

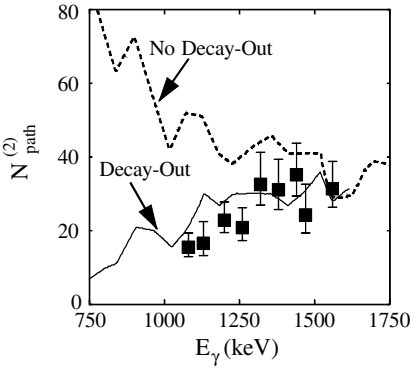

Fig. 2. The number of excited rotational bands obtained by the fluctuation analysis of the superdeformed ridge structures of ^{143}Eu, compared with cranked shell model calculations plus a two-body residual interaction including (solid line) or not (dashed line) the decay-out process into the normal deformed well. (Adapted from [2].)

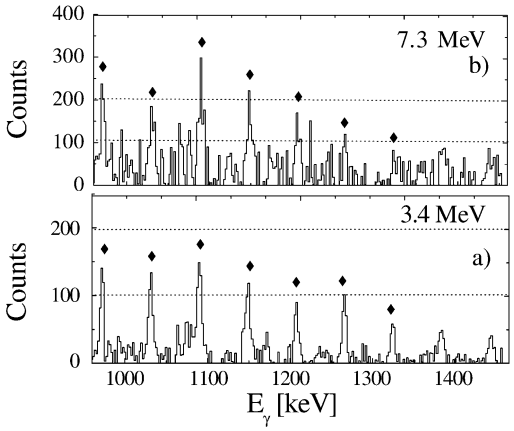

Fig. 3. Spectra of the SD yrast of ^{143}Eu, gated by high-energy γ-rays with average energies $\langle E_\gamma \rangle = 3.4$ (panel a)) and 7.3 MeV (panel b)). The spectra are normalized to the intensity of the low-spin 917 keV line, with the gating condition $\langle E_\gamma \rangle =$ 7.3 MeV. The diamonds indicate the SD lines used to calculate the increase of the yrast intensity. (Adapted from [8].)

analysis technique [16] is the effective number ($N^{(2)}_{\rm path}$) of excited rotational bands. The number $N^{(2)}_{\rm path}$ of paths available to the nucleus in the γ-decay through different regions of level density, namely the number of excited bands, as well as the effective number of damped transitions, can in fact be extracted from the simple relation $\mu_2/\mu_1 = N_{\rm eve}/N^{(2)}_{\rm path} + 1$ [16]. Here μ_1, μ_2 and $N_{\rm eve}$ are the first and second statistical moments and the number of counts in a $4/\mathcal{I}^{(2)} \times 4/\mathcal{I}^{(2)}$ sector, in which each rotational cascade contributes on the average one count, $\mathcal{I}^{(2)}$ being the dynamic moment of inertia of the nucleus.

The result obtained for the number of effective paths populating the ridge structure of ^{143}Eu is shown in fig. 2. The number of paths is found to depend very strongly on the transition energy, reaching a constant value of ≈ 30 bands in the region $1300 < E_\gamma < 1600$ keV. This corresponds to the transition energy region where the SD ridge is populated, following an intensity pattern similar to the SD yrast. At contrast, a continuous decrease is observed in the number of bands at lower transition energy [2]. A theoretical estimate of the effective number of discrete excited bands was obtained from the band mixing model [3,4] by counting the number of two consecutive transitions which branch out to less than two states. In fig. 2 two different band mixing calculations are shown, one without including any tunnelling from the SD to the ND minimum, and the other taking into account the decay-out mechanism as a function of excitation energy of the SD states [5,6], in a similar way as it has been done previously for the SD yrast band. This second model is found to reproduce remarkably well the experimental findings giving the first evidence that the decay-out mechanism is controlled by a quantum tunnelling through the barrier between the SD and ND minima, not only for the SD yrast but also for the SD excited bands.

5 Effect of E1 decay in the population of SD structures

A relevant open question concerning the problem of superdeformation is the understanding of the conditions which favor the population of SD states at the highest spins, as compared to the discrete line intensities observed in normally deformed nuclei at the same highest spin values [17,18]. It has been suggested that such intense population of the SD band at high spins can be related to the $E1$ feeding of these states, which is expected to be strongly affected by the shape of the giant dipole resonance (GDR) strength function in the low-energy tail (namely at E_γ lower than the neutron binding energy) [19]. This explanation was originally formulated in connection with the population of the SD nucleus ^{152}Dy [7]. To provide a very stringent experimental test of this mechanism, one needs to study the populations of the SD structures as a function of coincident high-energy γ-rays. In fact, in this way it is possible to verify whether or not the population of the SD structures increases with high-energy γ-ray gating, as expected from the GDR line shape built on a superdeformed nucleus. This is in general a difficult experimental task, due to both the exponential decrease of the yield of the high-energy γ-rays and to the weak intensity of the SD transitions, being of the order of few percent for the yrast band.

In order to address this problem, we have measured SD transitions (yrast and quasi-continuum) in coincidence with high energy γ-rays and we have studied the dependence of their intensity as a function of the high γ-ray energy in the interval 3–8 MeV [8]. This is the region where one can probe the low-energy tail of the GDR strength function, which, in the case of a SD prolate nucleus, is characterized by a double Lorentzian shape with one third of the strength expected to be around 10.5 MeV [19].

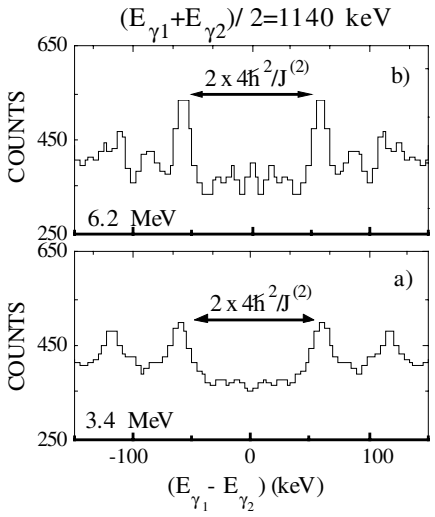

Fig. 4. Ridge structures at the average transition energy $(E_{\gamma_1} + E_{\gamma_2})/2 = 1140$ keV in the γ-γ matrix of ^{143}Eu, gated by high-energy transitions with $\langle E_\gamma \rangle = 3.4$ (panel a)) and 6.2 MeV (panel b)). The arrows indicate the separation between the two most inner ridges, corresponding to the moment of inertia of the SD yrast band. (Adapted from [8].)

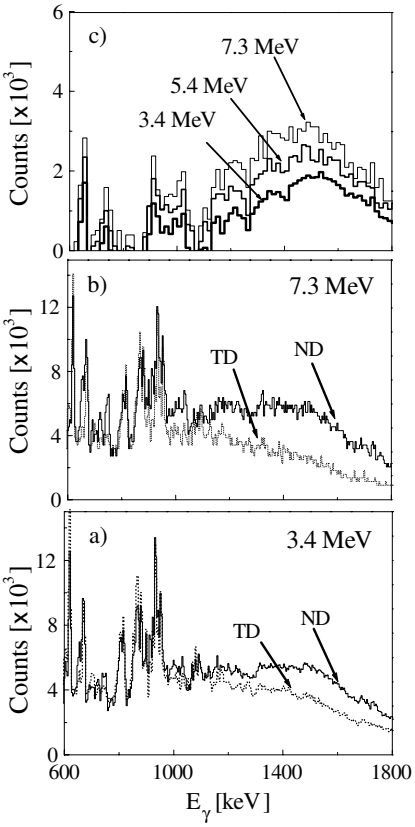

Fig. 5. Spectra of ^{143}Eu collecting the entire decay flow (ND) and the triaxial contribution only (TD), gated by high-energy transition with $\langle E_\gamma \rangle = 3.4$ (panel a)) and 7.3 MeV (panel b)). The intensity of the $E2$ bump observed in the ND spectra, obtained as a difference between the ND and TD spectra and normalized to the intensity of the 553 keV low-spin spherical transition, is shown in the top part (panel c)) of the figure. (Adapted from [8].)

The SD yrast band intensity is shown in fig. 3 for the following two gating conditions on the high-energy γ-ray detected in the BaF_2 scintillators: panel a) 3 MeV $< E_\gamma <$ 4 MeV with average energy $\langle E_\gamma \rangle = 3.4$ MeV and panel b) 6 MeV $< E_\gamma <$ 14 MeV with average energy $\langle E_\gamma \rangle = 7.3$ MeV. Each spectrum is also gated on low-energy SD yrast γ-rays, and Doppler-corrected by taking into account the energy-dependent fractional Doppler shift, as obtained by the DSAM analysis of the SD yrast band discussed in sect. 3. The spectra have been normalized to the intensity of the 917 keV low-spin transition between spherical states, to allow for a comparison of the superdeformed band population. The increase of the intensity with increasing high-energy gating, already visible in the figure, has been estimated by summing the intensity of the marked peaks. This has given a factor of 1.6 increase between the lowest and the highest gating condition, as discussed in connection with fig. 7 below.

The feeding properties of the superdeformed unresolved transitions, forming well-identified ridge-valley structures in $\gamma \times \gamma$ matrices (as discussed in the sects. 3 and 4), have also been studied. Figure 4 shows one-dimensional projections on a 60 keV wide strip perpendicular to the main diagonal of the $E_{\gamma 1} \times E_{\gamma 2}$ matrix at the average transition energy $(E_{\gamma 1} + E_{\gamma 2})/2 = 1140$ keV, for average high-energy gating transitions of $< E_\gamma >= 3.4$ and 6.2 MeV (panels a) and b), respectively). One can observe an enhancement of the ridge structure when measured in coincidence with transition of $E_\gamma > 6$ MeV, of the same order as observed for the SD yrast line.

In ^{143}Eu a continuous distribution of superdeformed character, corresponding to damped transitions at higher excitation energy, has also been observed in the region $1200 < E_\gamma < 1700$ keV [20]. It has been found that the intensity of such superdeformed $E2$ bump is much stronger for transitions leading to the population of the low-spin spherical (ND) structure as compared to that leading to the low-spin triaxial (TD) shape. Figure 5 shows the spectra emphasizing the region of the $E2$ continuum, normalized on the 553 keV low-spin spherical transition. To isolate in the best possible way the expected contribution from the superdeformed component only, we have evaluated the excess yield of the ND bump as compared to the TD bump, as shown in the top panel of fig. 5 [8]. Again, one clearly observes that the SD contribution to the continuum spectrum increases with the energy of the high-energy gate.

Figure 6 shows the results obtained for the relative intensity of the SD yrast transitions, as a function of the high-energy gating γ-ray. The intensity of triaxial (triangles) and spherical (circles) low-spin transitions is also shown in the same figure for comparison. While in the case of the SD yrast transitions the intensity deviates strongly from 1 at gating energy of 7.3 MeV, the same is not true for the spherical and triaxial cases. The simplest estimate of the increase population of the SD yrast can be deduced

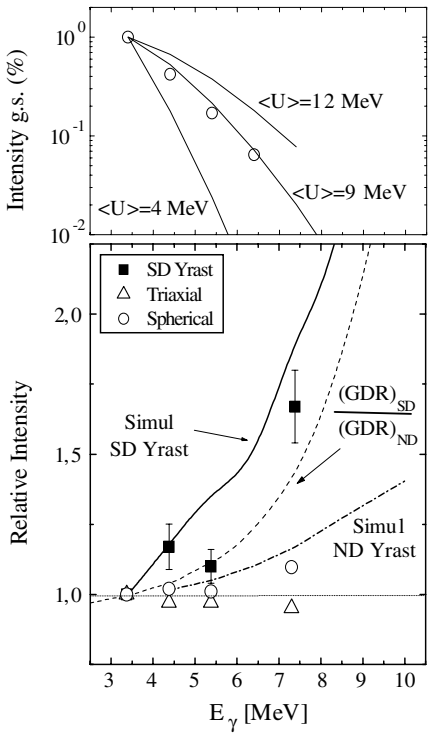

Fig. 6. The bottom part of the figure shows the relative intensities of the SD yrast band (squares) as a function of high-energy gating γ-rays, together with the relative intensity of the spherical (circles) and triaxial (triangles) low-spin transitions. The dashed line corresponds to the ratio of the strength functions of the GDR built on a SD and a ND nucleus, while the full (dashed-dot) line gives the predicted values of the relative intensity of the SD yrast (ground-state transition between spherical states), as obtained from the schematic model of refs. [7, 21]. The top part of the figure shows the measured relative intensity of the first-excited state to g.s. transition as a function of high-energy gating γ-rays, compared with the corresponding values obtained from the schematic model calculations at three different values of entry excitation energy.

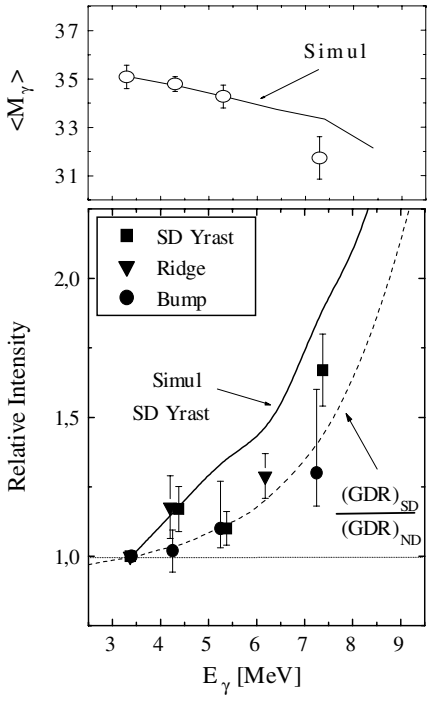

Fig. 7. The bottom part of the figure shows the intensity of the SD yrast (squares), of the SD ridge (filled triangles) and of the $E2$ bump (filled circles), as a function of the energy of the gating transition, relative to the corresponding values measured at $\langle E_\gamma \rangle = 3.4$ MeV. The dashed line corresponds to the ratio of the strength functions of the GDR built on a SD and a ND nucleus, while the full line gives the predicted values of the relative intensity of the SD yrast, as obtained from the model of refs. [7,21]. In the top part of the figure the total average multiplicity of the γ-cascades leading to ^{143}Eu is shown for both the experimental data (circles) and the model, as a function of the energy of the gating transition.

by calculating the ratio of the strength function of the superdeformed GDR ($E_{1\mathrm{GDR}} = 10.5$ MeV, $\Gamma_{1\mathrm{GDR}} = 3$ MeV with 33% of EWSR strength and $E_{2\mathrm{GDR}} = 17$ MeV, $\Gamma_{2\mathrm{GDR}} = 6.5$ MeV with 66% of EWSR) with the spherical GDR ($E_{\mathrm{GDR}} = 14.5$ MeV, $\Gamma_{\mathrm{GDR}} = 5$ MeV, 100% of EWSR), normalized to the data at 3 MeV, as shown by the dashed line.

To model in a more realistic way the complex γ-decay flow from the entry distribution of the residual nucleus down to the yrast line, we have also performed schematic Monte Carlo calculations. The adopted model has earlier been used to describe the populations of the various spectral component of the SD nucleus ^{143}Eu, giving a good account for the experimental data [21]. The model is based on the level densities of both ND and SD states, together with the $E1$ and $E2$ transition probabilities characteristic of the two deformed shapes. In the case of ND states, the level density is described by the Fermi-gas expression of ref. [22], with a level density parameter $a_{\mathrm{ND}} = A/10$, while the level density of SD states is taken from the cranking+band mixing calculations of ref. [3] (corresponding roughly to a level density parameter $a_{\mathrm{SD}} = A/18.6$). In the code, the two deformations are separated by a barrier, the tunnelling through which allows the mixing between SD and ND states. In particular, the statistical $E1$ strength entering into the simulation is described as the tail of the giant dipole resonance of Lorentzian shape, with centroids and widths for the SD and ND configurations, as given above.

The parameters used in the calculations are the same as discussed in ref. [21], with the only difference for the entry excitation energy, which was 4 MeV in the previous case and it has now been increased by 5 MeV to match the new experimental condition. This corresponds to an average entry energy of 9 MeV above yrast. In order to verify this condition, we have measured the variation of intensity of the first-excited state to g.s. transition as a function of high-energy gating γ-rays, and compared to the corresponding simulated values. The result is shown in the top panel of fig. 6, where one can see that indeed if one chooses an entry point of average energy 9 MeV, the relative intensity of the 917 keV transition from the first-excited state

to the ground state in ^{143}Eu is well reproduced by the simulation for high-energy gating γ-rays ranging from 3 to 8 MeV. The predicted intensity for the SD yrast and ND yrast deduced from this Monte Carlo model are shown in the lower panel of fig. 6 with the dot-dashed (ND) and full (SD) drawn lines. It is remarkable how well the simple model can reproduce not only the measured increase of the SD yrast but also the small positive deviation from 1 of the spherical transitions occurring at around $E_\gamma = 7.4$ MeV. This has been understood as due to the observation that the SD flux (ridges and $E2$ bump) depopulates through the spherical transitions mainly by-passing the triaxial deformation, which in fact shows a small decrease in intensity as a function of the high-energy γ-rays.

In fig. 7 we have summarized all results concerning the SD structures, by presenting in addition to the SD yrast data the results concerning the SD ridges and the $E2$ bump. Altogether, it is clear that the increase measured for the ridges and the $E2$ bump is consistent with that of the SD yrast, therefore supporting the SD nature of these structures. In order to rule out possible spin effects, for which we know that an increase of spin induces an increase of the population, we have measured the average multiplicity, which reflects the average spin, as a function of the high-energy gating γ-ray transition (top panel of fig. 7). In the present case, an opposite situation is found, since the increase of the SD population is observed to be associated with a decrease of the average spin of approximately 8 units, as deduced from the multiplicity measurement. It is also found that the value of the multiplicity deduced from the schematic Monte Carlo calculations reproduces rather well this observed decrease. In summary, one can say that we have found an increase of SD transition intensity and a decrease of the average γ-multiplicity with increasing high-energy γ-ray gates, which are both well reproduced by the same simulation calculations.

One can then conclude that the feeding intensity of the superdeformed states, including the damped transitions from the $E2$ continuum, is almost a factor of 1.6 larger when gating on high-energy γ-rays (with $E_\gamma > 6$ MeV) as compared to the ungated case. In fact, this not only clearly suggests that for ^{143}Eu the $E1$ decay is the favorable mechanism for the population of SD configurations, but also supports the superdeformed nature of the rotational quasi-continuum observed in this nucleus [20]. However, in order to see whether or not this is a general feature of the feeding of the SD structures, one needs more experimental work also in other regions of mass where superdeformed shapes have been found.

6 Conclusions

The study of excited states within the superdeformed well of the ^{143}Eu nucleus has provided the opportunity to investigate few intriguing aspects of nuclear structure in extreme conditions: the robustness of collectivity with increasing excitation energy and spin, and the role of the giant dipole resonance built on superdeformed states in the cooling process of the residual nuclei via emission of statistical dipole transitions. In particular, we have obtained three main interesting results:

i) the fact that ^{143}Eu maintains its collectivity and deformation with increasing excitation energy, as also observed in normally deformed nuclei [2];

ii) the first evidence that the decay-out mechanism is controlled, not only for the SD yrast but also for the SD excited bands, by a quantum tunnelling through the barrier between the SD and ND minima [2];

iii) for ^{143}Eu the $E1$ decay is the favorable mechanism for the population of SD configurations, also supporting the superdeformed nature of the rotational quasi-continuum observed in this nucleus [8].

It is planned for the near future to investigate further the problem of survival of superdeformation at high excitation energy both by studying the quasi-continuum and the GDR in other mass regions. This will allow to obtain a clearer and more consistent picture on this interesting and rather unexplored problem.

We wish to acknowledge the support from INFN, Italy, from the Danish Natural Science Research Council, from the Polish Scientific Committee (KBN Grant No. 2P03B11822) and the EU Access to Large Scale Facilities-Training and Mobility of Research Program Contract No. ERBFMGECT980110, for INFN-Laboratori Nazionali di Legnaro.

References

1. E. Vigezzi *et al.*, Phys. Lett. B **249**, 263 (1990).
2. S. Leoni *et al.*, Phys. Lett. B **498**, 137 (2001).
3. K. Yoshida, M. Matsuo, Nucl. Phys. A **612**, 26 (1997).
4. K. Yoshida, M. Matsuo, Nucl. Phys. A **636**, 169 (1998).
5. K. Yoshida, M. Matsuo, Y.R. Shimizu, Nucl. Phys. A **696**, 85 (2001).
6. Y.R. Shimizu, M. Matsuo, K. Yoshida, Nucl. Phys. A **682**, 464c (2001).
7. B. Herskind *et al.*, Phys. Rev. Lett. **59**, 2416 (1987).
8. G. Benzoni *et al.*, Phys. Lett. B **540**, 199 (2002).
9. A. Winther, Nucl. Phys. A **594**, 203 (1995).
10. J. Simpson, Heavy Ion Phys. **6**, 253 (1997).
11. A. Maj *et al.*, Nucl. Phys. A **571**, 185 (1994).
12. S.A. Forbes *et al.*, Nucl. Phys. A **584**, 149 (1995).
13. M. Piiparinen *et al.*, Phys. Rev. C **52**, R1 (1995).
14. B. Million *et al.*, Phys. Lett. B **415**, 321 (1997).
15. S. Frattini *et al.*, Phys. Rev. Lett. **81**, 2659 (1998).
16. T. Døssing *et al.*, Phys. Rep. **268**, 1 (1996).
17. K. Schiffer, B. Herskind, J. Gascon, Z. Phys. A **332**, 17 (1989).
18. J. Simpson *et al.*, Phys. Rev. C **62**, 024321 (2000).
19. M. Gallardo *et al.*, Nucl. Phys. A **443**, 415 (1985).
20. S. Leoni *et al.*, Phys. Rev. Lett. **76**, 3281 (1996).
21. S. Leoni *et al.*, Phys. Lett. B **409**, 71 (1997).
22. S. Aberg, Nucl. Phys. A **477**, 18 (1988).